

OriSnake: Design, Fabrication, and Experimental Analysis of a 3-D Origami Snake Robot

Ming Luo¹, Ruibo Yan, Zhenyu Wan¹, Yun Qin, Junius Santoso¹, Erik H. Skorina¹, and Cagdas D. Onal¹

Abstract—Snake robots offer a useful and unique mobility platform for search-and-rescue applications. However, existing prototypes made of rigid links and joints are hampered by a lack of flexibility that limits their utility in highly cluttered, maze-like environments, and their heavy weight limits their energy-efficiency and performance in three-dimensional (3-D) tasks. To address these challenges, this letter presents a new approach using cylindrical, origami continuum modules driven by internal cables and electric motors, as well as a local feedback control system on each module. Thus, we can distribute actuation, sensing, and control for highly scalable soft robotic continuum origami systems. Using this approach, we develop a 3-D origami robotic snake that is able to locomote using lateral undulation and sidewinding gaits similar to those used by biological snakes. The proposed snake robot is a continuously deformable, lightweight, modular, and low cost robotic system made of a folded thin plastic body. We detail the design, fabrication, and control of this first 3-D origami robotic snake prototype, focusing on the analysis of locomotion parameters for each gait. We experimentally search for the optimal parameters for both types of locomotion, with maximum speeds characterized as 40.5 mm/s (0.1 body-lengths per second) for lateral undulation and 35 mm/s (0.09 body-lengths per second) for sidewinding locomotion.

Index Terms—Flexible robotics, biologically-inspired robots, compliant joint/mechanism.

I. INTRODUCTION

Snake robots represent an ideal robotic platform for search-and-rescue applications, as well as tasks in constrained and hazardous environments. The simple structure of the snake body has the capability to traverse complex, constrained, 3-D environments. Snakes are capable of fitting through small gaps, moving over rough terrain, and climbing shear inclines, all of which are useful to navigate the dense undergrowth of a forest or the wreckage of a collapsed building.

A range of snake robots have been developed using traditional robotic kinematics comprising rigid links and discrete joints. Wright *et al.* developed a simple, modular snake robot made of servo motors mounted in series, capable of climbing up

the inside of a pipe [1]. Crespi *et al.* developed a larger, more complex snake robot with DC motors and detachable wheels capable of locomotion on land and in water [2]. Snake robots can use different methods of locomotion, including most frequently serpentine locomotion (or lateral undulation) and sidewinding locomotion [3]–[6].

Rigid robotic snakes, though capable of snake-like motion [7], [8], suffer from a number of problems. The fact that rigid snakes only articulate at discrete points mean that they can only approximate the smooth continuum body motions of biological snakes by many small links operated in coordination. This may reduce the effectiveness of their locomotion, increase energy consumption, control complexity, and can make it difficult to access unpredictable and highly-constrained environments targeted for snake robot operation.

To address this problem, our prior work focused on developing soft pressure-operated robotic snakes [9], [10]. These soft robotic snakes use pneumatic pressure to actuate silicone rubber segments that make up the body of the snake, resulting in a constant-curvature deformation along the length of each segment. This results in a flexible, safe, and realistic motion, effectively mimicking the gait of a biological snake.

Unfortunately, soft pneumatic actuators also have disadvantages. They can be inefficient, constantly venting their motive pressure to the environment. In addition, the compressors required to generate the input pressure used in pneumatic actuators tend to be heavy and bulky, reducing the effectiveness of this type of actuation for autonomous mobile robotic applications.

In this letter, we introduce a self-contained, lightweight, low cost and flexible origami robotic snake (OriSnake). OriSnake is constructed of origami modules that resemble bellows and actuated via cables connected to electric motors. Thus, we combine the flexibility of soft robotics and the portability and efficiency of traditional electrical actuation.

Origami is the Japanese art of creating structures and objects by folding paper. Taking inspiration from this technique, we can create structures and mechanisms that are both flexible and light-weight [11]. Recently, Zhang *et al.* created a cable-driven continuum bending actuator with an origami shell and a helical spring core [12]. Of particular relevance to our work, Vander *et al.* created a cable driven origami robot used for both continuum bending manipulation and locomotion [13], which consisted of a single module using an inch-worm style gait. This gait is both dependent on the frictional properties of the environment and tends to be very slow, with the resulting origami mobile robot only capable of a locomotion speed about 6 mm/s.

Manuscript received September 10, 2017; accepted January 12, 2018. Date of publication January 31, 2018; date of current version March 21, 2018. This letter was recommended for publication by Associate Editor Y. Ou and Editor Y. Sun upon evaluation of the reviewers' comments. (Ming Luo and Ruibo Yan contributed equally to this work.) (Corresponding author: Cagdas D. Onal.)

The authors are with the Mechanical Engineering Department and Robotics Engineering Program, Worcester Polytechnic Institute, Worcester, MA 01609 USA (e-mail: mluo@wpi.edu; ryan2@wpi.edu; zwan@wpi.edu; yqin@wpi.edu; jsantoso@wpi.edu; ehskorina@wpi.edu; cdonal@wpi.edu).

Digital Object Identifier 10.1109/LRA.2018.2800112

Paez *et al.* presented a design of a modular origami snake robot in [14] and created the origami framework, but did not incorporate any actuation.

We discussed the initial design of continuum origami modules for manipulation applications in our previous work, demonstrating their high torsional strength and controllability [11], [15]. Each module is self contained and capable of collapsing itself to a fraction of its original length. Taking cues from our previous expertise in soft robotic snakes [16], this work combines the advantages of soft robotics and origami-inspired design and fabrication, to present a new robotic platform we call WPI Origami Robotic Snake (OriSnake).

OriSnake, shown in Fig. 1, consists of four origami continuum modules mounted in series. Each module has its own slave controller, allowing for easy repair and modification of the OriSnake prototype. The plastic sheet used in these modules provides a compliant, highly deformable structure, while the origami structure provides stiffness in the desired, torsional direction. Each module has two degrees of bending freedom, allowing each module to bend off the ground. This type of motion is required for a sidewinding gait and allows the snake to operate in non-planar environments. Thus, we refer to it as a “3-D” snake, to contrast it with existing soft, planar snakes. Each module includes passive wheels, which provide the anisotropic friction required for the lateral undulation method of snake locomotion. We describe a simple but effective suspension mechanism to ensure that each passive wheel makes contact with the ground for lateral undulation.

We show through experimentation that the WPI OriSnake is capable of both lateral undulation and side-winding. In addition, we analyze the behavior of the OriSnake under different locomotion parameters and search for optimal set of parameters for maximum linear speed for both locomotion gaits.

This work represents:

- A 3-D soft robotic snake,
- An origami snake robot, and
- The demonstration and analysis of side-winding locomotion gait in a soft robotic snake.

II. ORIGAMI ROBOTIC SNAKE DESIGN

A. Module Design

The WPI Origami Robotic Snake was constructed out of origami continuum bending modules based on our previous work [15]. The flexible mechanism of these modules consists of the Yoshimura pattern: a bellows-like origami crease pattern, as shown in Fig. 2. This mechanism is constructed out of three pieces of laser-machined 7 mil thick folded plastic (PET) (following our origami fabrication process [11], [15]). The modules can bend, contract, and extend, while inherently resisting torsional deformation. The origami body connects between a sheet of 1/8” thick laser-cut acrylic on one end and a local module control board on the other. Each module is 66 mm long when un-actuated, and the acrylic plate has a maximum radius of 52 mm.

The module control board has mounts for three N 20 gear DC motors (gear ratio 1:150) to actuate each module. These motors have 3-D printed spools on their output shafts, which



Fig. 1. The 3D origami snake robot.

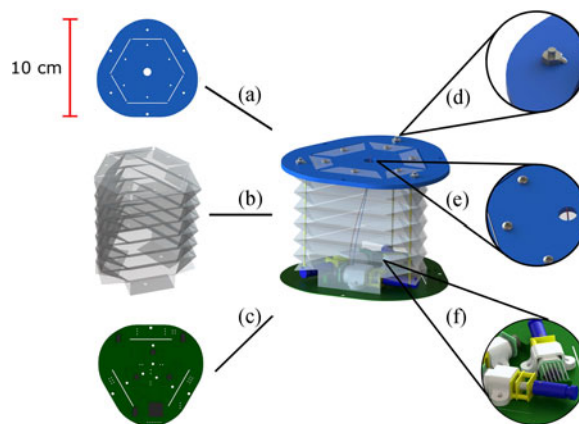


Fig. 2. The individual modules used to construct the OriSnake. (a) Acrylic Plate, (b) 3-part origami bellows, (c) control board, (d) cable mounting screw, (e) bellows mounting screws, (f) interior motor mounts.

are connected to nylon fishing lines as cables. These cables are attached to the acrylic plate on the other end of the module. As a motor retracts its cable, the module bends in the direction of the cable. The motors and cables are mounted in a triangular pattern, giving each module a full 3 degrees-of-freedom (DoF). The cables are fed through a series of holes in the origami crease pattern, keeping them in position and maximizing the bending moment they can apply to the module. An inherent axial stiffness of the Yoshimura pattern provides antagonism to keep the cables in tension without additional components. Each control board is independent, able to read encoder data from each of the motors and able to perform low-level feedback control on each of its cable lengths (as described in Section III). The hollow nature of the origami body allows cables transferring power and information to be easily slotted through, protecting them from potential external contact. In order for lateral undulation to function properly, a snake (or a snake robot) needs the tangential friction to be considerably less than the normal friction (lateral to the body axis) at its ground contact points. To provide this anisotropic friction requirement, passive wheels were added to the bottom of each module, as common for snake robots. These wheels are unpowered (passive), and only serve to mimic the frictional properties of snake skin, which exhibit large friction in the lateral direction and low friction in the longitudinal direction

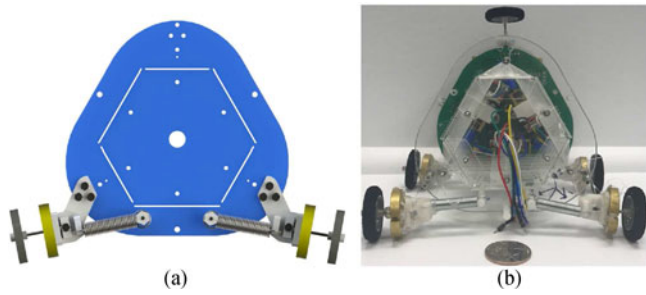


Fig. 3. The suspension system of each module. (a) CAD model. (b) Prototype. The suspension system keeps the wheels in contact with the ground as the modules bend, increasing the effectiveness of the serpentine locomotion.

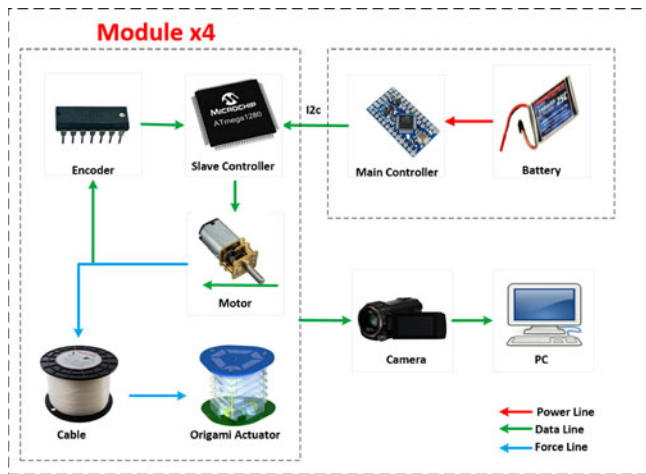


Fig. 4. System architecture of the OriSnake robot. It consists of a master controller and battery, which drive and communicated the 4 modules that make up the body of the snake. Each module performs low-level PID control on each motor. A motion tracking system is used to record the state of the OriSnake for verification purposes.

with respect to the long axis of the slender body. Because of fabrication inconsistencies and control offsets between modules, we observed that not all of the wheels were able to touch the ground during the various stages of the gates. This reduced or eliminated their anisotropic friction properties, and drastically reduced the performance of the OriSnake. To achieve a more uniform load distribution on the wheels, we added a simple suspension system on each wheel, shown in Fig. 3, which helped the snake robot locomote with continuous ground contact and desirable friction properties for lateral undulation. In addition, we observed that the body is too light for secure contact with the ground. Hence, we added 20 g weights at each wheel, as well as additional weights at the head and tail. This also helped keep the wheels on the ground, as the origami body is too strong and light to stay in contact with the ground. Thus, we expect that the OriSnake can carry significant payload for real world applications in the future.

B. System Architecture

Fig. 4 depicts the system architecture of the WPI OriSnake, with a master controller and 4 modules, which is the minimum number of modules required for lateral undulation [7]. In total,

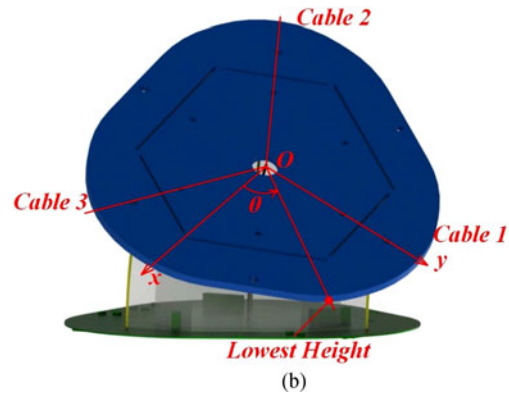
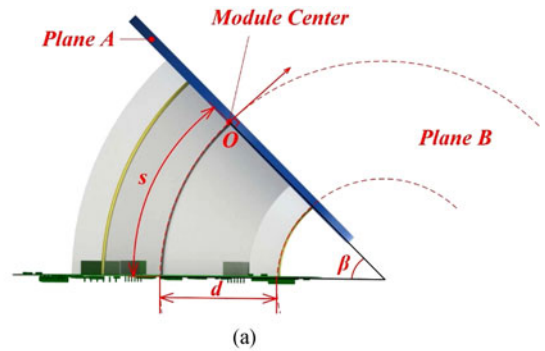


Fig. 5. (a) shows the bending angle of the single module. β is the bending angle between the top plate and bottom plate. (b) shows to which direction the module is bending. In xy plane of the top plate, the line connecting the center O and cable 1 is the y axis. The line between the center and the lowest point represents the direction in which the module is bending. The bending angle θ is the angle between direction line and x-axis of the top plate.

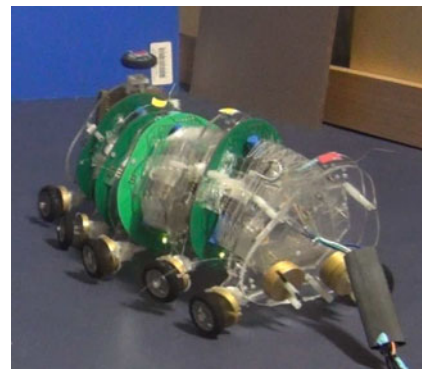


Fig. 6. The OriSnake performing sidewinding locomotion by forming a traveling helical wave, which periodically lifts its wheels off the ground.

the length of the OriSnake is 380 mm. Because it is a modular system, each bending module has an independent slave controller, which performs all low-level joint control actions. The purpose of the low-level control is to modulate the motors to pull or release cables so the module will deform as combinations of the three cable lengths. Each slave controller performs three simple functions. First, it will receive instructions from high level controller over an I2C communication bus. Second, it reads encoder values for each motor. Finally, it calculates and outputs the corresponding PWM commands for the motors.

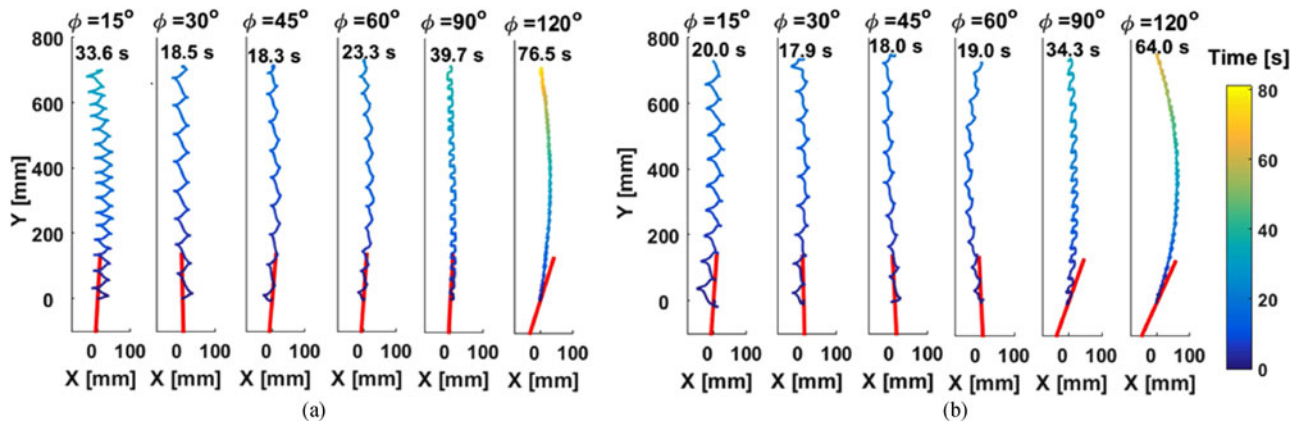


Fig. 7. The Center of Mass (CoM) trajectory of the snake robot during serpentine locomotion. Offset $\phi = 15^\circ, 30^\circ, 45^\circ, 60^\circ, 90^\circ, 120^\circ$. Trajectories are noted for more concise plotting, with the initial position of the snake shown with red lines. The colorbar on the right shows the time of each data point, with the final time shown for each trajectory. (a) The amplitude angle $\beta = 60^\circ$ (b) The amplitude angle $\beta = 45^\circ$.

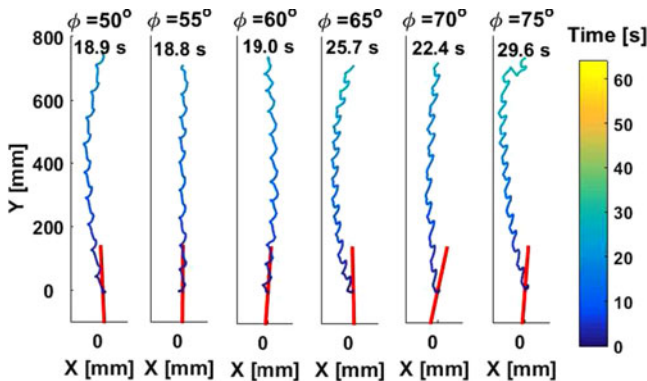


Fig. 8. The Center of Mass (CoM) trajectory of the snake robot during serpentine locomotion for $\beta = 45^\circ$ and offset $\phi = 50^\circ, 55^\circ, 60^\circ, 65^\circ, 70^\circ, 75^\circ$. Trajectories were rotated for more concise plotting, with the initial pose of the snake indicated by red lines. The colorbar on the right shows the time of the data point, with the final time shown for each trajectory.

The master controller (Arduino Pro Mini) and one battery, located at the head of the snake, sends commands to each slave controller using I2C serial communication. We used an external power supply to drive the motors for convenience, but this is not a limitation on the self-contained performance of the robot. We placed color markers on each bending module, which allowed an external camera to track the position in the experiment for analysis.

III. CONTROL SCHEME

To help in understand the control algorithms, Table I lists the kinematic parameters needed to specify the locomotion gaits. For additional clarification, Fig. 5 shows the definitions of geometric parameters, especially the angles β and θ , which represent the bending angle and bending plane orientation for a given module.

Both gait selection and low-level control algorithms are executed on the distributed slave controllers. The speed of the control loop is around 0.006 s. The master controller, an Arduino Pro Mini, makes sure that the control algorithm is executed

TABLE I
KINEMATIC PARAMETERS OF WPI ORISNAKE

β	bending angle between the top plate and bottom plate
θ	angle of bending direction and x -axis in top plate
ω	the angular velocity of theta
ϕ	phase offset between two adjacent modules
s	neutral-axis length of each module
κ_i	curvature of the neutral axis of module i
d	distance between the center of plate to each cable
L_{jd}	the desired length of each cable j
L_{jc}	the current length of each cable j

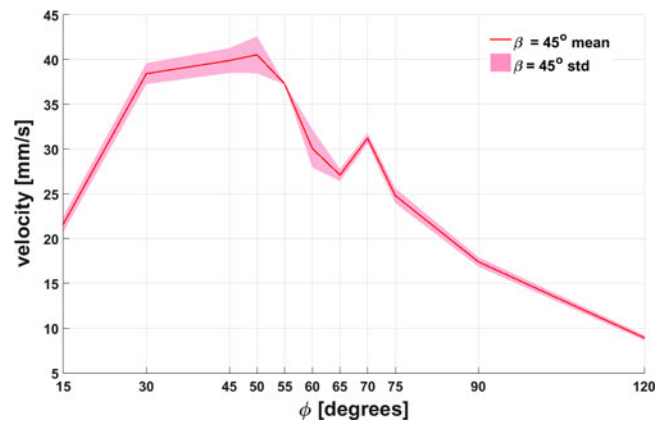


Fig. 9. The mean and standard deviation of the velocity of the center of mass of the OriSnake with $\beta = 45^\circ$ for varying offset angles ϕ on the horizontal axis. The results were calculated using 3 separate experiments.

synchronously on the slave controllers by sending a time signal over the I2C bus during operation.

The snake robot has two locomotion modes: serpentine (or lateral undulation) and side-winding. In serpentine locomotion, the snake robot oscillates left and right in the horizontal plane, propelled forward by the anisotropic friction of its wheels. The control formulation of this type of gait is as follows:

$$\kappa_i(t) = \frac{\beta}{s} \sin(\pi t + i\phi) \quad (1)$$

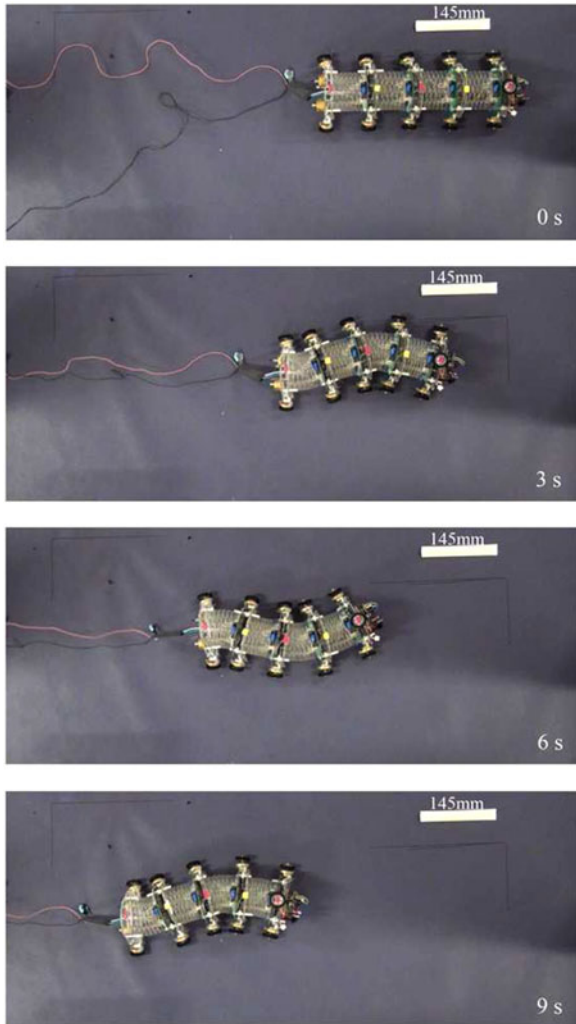


Fig. 10. Top view snapshots of lateral undulation gait over 9 seconds for $\beta = 45^\circ$ and $\phi = 70^\circ$.

The period of the gait is fixed at 2 seconds, because this is the fastest undulation frequency that will allow the modules to bend to a full 60° (their maximum range) with the given motors.

From (1) we can calculate the curvature κ of each module, where i is the number of module starting from 0. Each module follows a sinusoidal curvature wave with an offset of $i\phi$, thus generating a traveling wave. In the OriSnake prototype, we install the wheels along the lines from center to Cable 2 and Cable 3 which makes the x -axis of the top plate point horizontally right. As mentioned in the module design part, the body weight is not enough to make the modules bend in the horizontal direction and provide a downward force at the same time. To increase the downward force, we modified the bending planes so that for positive curvatures $\theta = 187^\circ$ (instead of 180) and for negative curvatures $\theta = 353^\circ$ (instead of 0). This makes the modules bend 7 degrees towards the ground, ensuring proper contact. For this locomotion gait, we analyze the effect of the parameter $\beta = 45^\circ, 60^\circ$ and the effect of the phase offset ϕ .

For sidewinding locomotion, the snake does not need to rely on its anisotropic friction. Instead, it physically lifts parts of

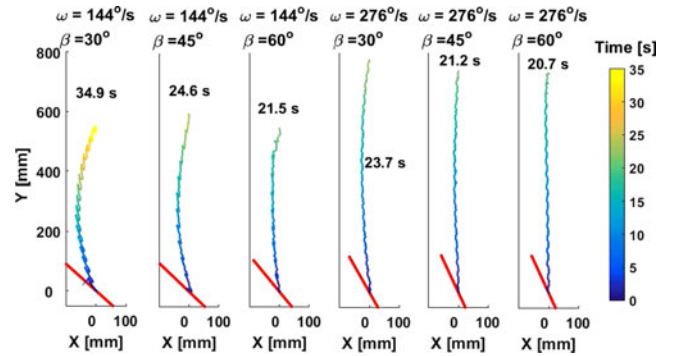


Fig. 11. The Center of Mass (CoM) trajectory of the snake robot during sidewinding locomotion. The offset $\beta = 30^\circ, 45^\circ, 60^\circ$ and the angular velocity $\omega = 144^\circ/s, 276^\circ/s$. Trajectories are rotated to improve the visualization, with the initial pose of the snake shown as a red line. The colorbar on the right shows the time of the data point, with the final time shown for each trajectory.

its body off the ground, as though making a stepping motion (Fig. 6). In this unique locomotion gait, the snake body forms a helical shape and moves to turn the helix from head to tail, causing a diagonal motion [17]. To realize this in the OriSnake, we have each module maintain a constant curvature (β) while changing θ at constant angular velocity from 0 to 360° . The desired angle of each module is offset from the ones adjacent to it in order to generate a traveling wave with $\phi = 90^\circ$, which creates the overall sidewinding motion. For the WPI OriSnake prototype, we explored two angular velocities $\omega = 144^\circ/s$ or $276^\circ/s$. The module will complete one full rotation in around 2.5 s when $\omega = 144^\circ/s$ and approximately 1.25 s when $\omega = 276^\circ/s$. In addition, we analyzed two bending angles for $\beta = 45^\circ, 60^\circ$.

For a rigid snake robot, sidewinding motion is generated with a combination of different equations for lateral and vertical joint angles [17]. To simplify this, and taking advantage of our 3-DoF continuously deformable modules, we set a constant bending curvature and a phase offset for each module, which will generate a helical shape. When we adjust the θ values, we effectively rotate the helix, and propel the snake for sidewinding locomotion.

For given $\kappa(t)$ and β values, we use inverse kinematic equations to calculate the cable lengths L_{1d} , L_{2d} , and L_{3d} as follows [15]:

$$\begin{aligned}
 L_{1d} &= 2\sin\left(\frac{\kappa S}{2}\right)\left(\frac{1}{\kappa} - d\sin(\theta)\right) \\
 L_{2d} &= 2\sin\left(\frac{\kappa S}{2}\right)\left(\frac{1}{\kappa} + d\sin\left(\frac{\pi}{3} + \theta\right)\right) \\
 L_{3d} &= 2\sin\left(\frac{\kappa S}{2}\right)\left(\frac{1}{\kappa} - d\cos\left(\frac{\pi}{6} + \theta\right)\right)
 \end{aligned} \tag{2}$$

For low-level feedback control, each slave control board will use PID to drive the cables to the desired lengths according to these equations.

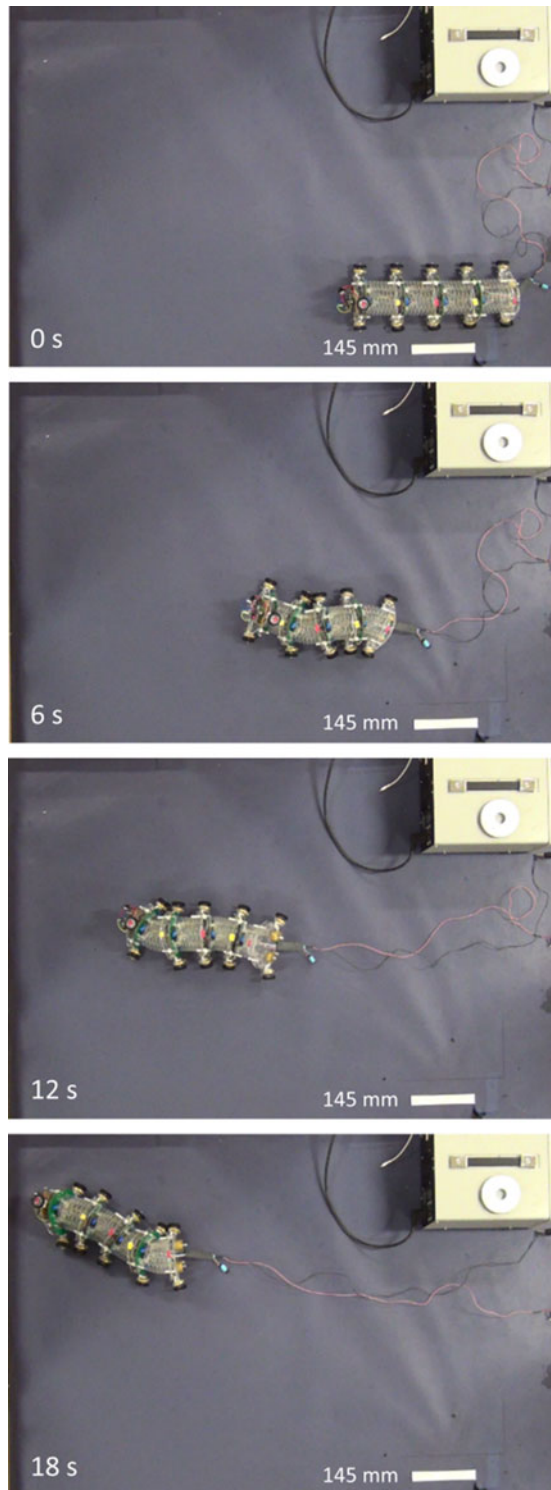


Fig. 12. Top view snapshots of sidewinding gait over 18 seconds for $\beta = 60^\circ$, $\omega = 144^\circ/\text{s}$.

IV. EXPERIMENTAL RESULTS

A. Lateral Undulation

We performed a range of experiments, investigating the performance of the OriSnake using different gait parameters for both lateral undulation and sidewinding locomotion modes. For

TABLE II
THE LINEAR VELOCITY OF THE ORISNAKE FOR VARYING SIDEWINDING PARAMETERS

$\omega \backslash \beta$	30°	45°	60°
$144^\circ/\text{s}$	$16.0 \pm 1.1 \text{ mm/s}$	$24.0 \pm 2.4 \text{ mm/s}$	$26.4 \pm 3.3 \text{ mm/s}$
$276^\circ/\text{s}$	$33.4 \pm 2.2 \text{ mm/s}$	$34.9 \pm 0.5 \text{ mm/s}$	$33.8 \pm 3.5 \text{ mm/s}$

lateral undulation, we tested locomotion offsets ϕ from 15° to 120° with amplitude angle $\beta = 45^\circ$ and 60° . Representative trajectories from these experiments can be seen in Fig. 7. From the results, we can see that the CoM trajectory is generally faster and more linear when $\beta = 60^\circ$. In addition, the maximum CoM linear velocity occurs when $\phi = 45^\circ$ for both $\beta = 45^\circ$ and $\beta = 60^\circ$.

We performed a finer-resolution search between $\phi = 45^\circ$ and $\phi = 75^\circ$ in order to get a better idea of the maximum performance of the OriSnake. Fig. 8 shows representative trajectories from this, while Fig. 9 shows the mean and standard deviation values for the linear velocity of the prototype, indicating repeatable results. These figures show that $\phi = 50^\circ$ results in the maximum linear velocity, reaching around 40.5 mm/s . Fig. 10 shows representative snapshots of a lateral undulation experiment for the parameters $\beta = 45^\circ$ and $\phi = 70^\circ$.

B. Sidewinding

We also performed similar experimental performance analyses with the sidewinding gait. We tested locomotion offsets of $\phi = 30^\circ$, 45° , 60° and the angular velocities (of the bending plane orientation θ) $\omega = 144^\circ/\text{s}$, $276^\circ/\text{s}$, the results of which can be seen in Fig. 11. From these results, we can see that the CoM trajectory is more linear than with the serpentine locomotion for all ranges of inputs, despite the body making a diagonal motion as caused by the sidewinding gait. In addition, the maximum CoM linear velocity is found (among the parameters investigated) when locomotion offset $\beta = 45^\circ$ and $\omega = 276^\circ/\text{s}$ as shown in Table II. Fig. 12 displays representative snapshots of the WPI OriSnake performing sidewinding locomotion using parameters $\beta = 45^\circ$, $\omega = 144^\circ/\text{s}$.

V. CONCLUSION

This article introduced the WPI Origami Robotic Snake (WPI OriSnake) that is capable of executing both lateral undulation (serpentine) and sidewinding locomotion modes. This robot is a low-cost, lightweight, modular system, where each module has its own slave controller, distributed sensing, and actuation. We performed experiments with the OriSnake, and found that a maximum velocity of 40 mm/s (0.1 body-lengths-per-second) could be achieved during serpentine locomotion, but that sidewinding could also be achieved with a maximum velocity of 35 mm/s (0.09 body-lengths-per-second).

In this work the OriSnake used an external power supply to drive the motors. This was mainly done for the sake of simplicity to control the maximum current during testing. The use of on-board batteries is unlikely to be detrimental to the performance

of the snake. In fact, during initial testing, we found that the snake was too light. This is partially caused by the high torsional stiffness of the origami modules. When a module has a slight rotation around its axis or at its end-plates due to imperfections in fabrication, the torsional stiffness of the module would be too high for the next module to fully make contact with the ground. This was particularly a factor in serpentine locomotion, and the additional weight of on-board batteries might actually increase performance.

In future work, we plan to optimize the mechanical design of this snake robot. The velocity of the current snake robot is slow compared to other snake robots. One cause of this is that the current gear motors we used are able to generate large torques, but with a much slower velocity. Additional work can be done to choose a motor that has the speed and torque capabilities to make the OriSnake faster while still having a small enough profile to fit inside the modules. This can be combined with a replacement for the passive wheels to bring the OriSnake closer to studies in real-world search-and-rescue.

We believe that the unique combination of the low-cost and lightweight origami-inspired design and manufacturing, with soft robotic locomotion offers advantages in applications that require robots to go through tight passages and navigate cluttered environments autonomously without tethers. The fact that the OriSnake can lift its modules off the ground means it can operate in 3-D environments. We plan to study these conditions, and examine the efficacy of our gaits on rough terrain. For example, the serpentine gait can go faster in some environments, like the one tested in this letter, but the sidewinding gait is likely to be more versatile. Future work will include motion planning and decision making algorithms, which will need to take these and other complex factors into account.

REFERENCES

- [1] C. Wright *et al.*, "Design of a modular snake robot," in *Proc. IEEE/RSJ Int. Conf. Intell. Robots Syst.*, 2007, pp. 2609–2614.
- [2] A. Crespi and A. J. Ijspeert, "Amphibot ii: An amphibious snake robot that crawls and swims using a central pattern generator," in *Proc. 9th Int. Conf. Climbing Walking Robots*, no. BIOROB-CONF-2006-001, 2006, pp. 19–27.
- [3] S. Hirose and M. Mori, "Biologically inspired snake-like robots," in *Proc. ROBIO 2004. IEEE Int. Conf. Robot. Biomimetics*, 2004, pp. 1–7.
- [4] F. Matsuno and K. Suenaga, "Control of redundant 3d snake robot based on kinematic model," in *Proc. IEEE Int. Conf. Robot. Autom.*, 2003, vol. 2, pp. 2061–2066.
- [5] K. L. Paap, T. Christaller, and F. Kirchner, "A robot snake to inspect broken buildings," in *Proc. 2000 IEEE/RSJ Int. Conf., Intell. Robots Syst.*, 2000, vol. 3, pp. 2079–2082.
- [6] Z. Bing, L. Cheng, G. Chen, F. Röhrbein, K. Huang, and A. Knoll, "Towards autonomous locomotion: Cpg-based control of smooth 3d slithering gait transition of a snake-like robot," *Bioinspiration Biomimetics*, vol. 12, no. 3, 2017, Art. no. 035001.
- [7] P. Liljebäck, K. Y. Pettersen, O. Stavdahl, and J. T. Gravdahl, *Snake Robots: Modelling, Mechatronics, and Control*. New York, NY, USA: Springer-Verlag, 2012.
- [8] S. Ma, N. Tadokoro, B. Li, and K. Inoue, "Analysis of creeping locomotion of a snake robot on a slope," in *Proc. IEEE Int. Conf., Robot. Autom.*, 2003, vol. 2, pp. 2073–2078.
- [9] C. Onal and D. Rus, "Autonomous undulatory serpentine locomotion utilizing body dynamics of a fluidic soft robot," *Bioinspiration Biomimetics*, vol. 8, no. 2, 2013, Art. no. 026003.
- [10] M. Luo *et al.*, "Slithering towards autonomy: A self-contained soft robotic snake platform with integrated curvature sensing," *Bioinspiration Biomimetics*, vol. 10, no. 5, 2015, Art. no. 055001.
- [11] C. D. Onal, R. J. Wood, and D. Rus, "An origami-inspired approach to worm robots," *IEEE/ASME Trans. Mechatronics*, vol. 18, no. 2, pp. 430–438, Apr. 2013.
- [12] K. Zhang, C. Qiu, and J. S. Dai, "An extensible continuum robot with integrated origami parallel modules," *J. Mech. Robot.*, vol. 8, no. 3, 2016, Art. no. 031010.
- [13] E. Vander Hoff, D. Jeong, and K. Lee, "Origamibot-i: A thread-actuated origami robot for manipulation and locomotion," in *Proc. 2014 IEEE/RSJ Int. Conf., Intell. Robots Syst.*, 2014, pp. 1421–1426.
- [14] L. Paez, M. Granados, and K. Melo, "Conceptual design of a modular snake origami robot," in *Proc. 2017 IEEE Int. Symp. Safety, Security, Rescue Robot.*, pp. 1–2, 2013.
- [15] J. Santoso, E. Skorina, M. Luo, R. Yan, and C. D. Onal, "Design and analysis of an origami continuum manipulation module with torsional strength," in *Proc. IEEE/RSJ Int. Conf. Intell. Robots Syst.*, 2017, pp. 2098–2104.
- [16] M. Luo, F. Chen, E. Skorina, W. Tao, Y. Sun, and C. Onal, "Motion planning and iterative learning control of a pressure-operated modular soft robotic snake," *Trans. Mechatronics*, Under Review.
- [17] M. Tesch *et al.*, "Parameterized and scripted gaits for modular snake robots," *Adv. Robot.*, vol. 23, no. 9, pp. 1131–1158, 2009.